

A comparative study of the contrast of solar magnetic elements in CN and CH

V. Zakharov¹, A. Gandorfer¹, S. K. Solanki¹, and M. Löfdahl²

¹ Max-Planck-Institut für Sonnensystemforschung, Max-Planck-Strasse 2, 37191 Katlenburg-Lindau, Germany
email: zakharov@linmpi.mpg.de, solanki@linmpi.mpg.de, gandorfer@linmpi.mpg.de

² Stockholm Observatory, Swedish Royal Academy of Sciences, S-13336 Saltsjöbaden, Sweden
email: mats@astro.su.se

Received; accepted

Abstract. Photospheric bright points were investigated in three different wavelength bands using interference filters centered at 436.5 nm (continuum), 430.5 nm (Fraunhofer's G-band dominated by absorption due to CH), and 388.7 nm (absorption band of CN). Such bright points serve as proxies of small-scale solar magnetic elements. Near diffraction limited imaging was achieved by real-time frame selection and subsequent joint phase diversity speckle reconstruction.

Comparison of the filtergrams of NOAA0670 taken in CH and CN shows that the contrast of bright points is on average 1.3 times higher in CN than in G-band, which is in good quantitative agreement with the predictions of Berdyugina et al. (2003).

Key words. Sun: activity – Sun: faculae, plages – Sun: magnetic fields

1. Introduction

High resolution filtergrams of the solar surface taken in the G-band at around 430.5 nm, dominated by an absorption band of CH, show bright features in the intergranular regions. Although these structures are often elongated along the narrow intergranular lanes, the name intergranular bright points (BP) has been used ever since BPs were first observed in 1984 (Muller & Roudier 1984). Since then a number of observations and theoretical investigations of their radiative properties have been carried out (e.g. Berger & Title 1996; Löfdahl et al. (1998); Langhans et al. 2002). Intergranular bright points show a strong spatial correlation with magnetic flux concentrations and are therefore useful as magnetic proxies, which allow the distribution and dynamics of magnetic features to be studied at higher spatial resolution than using spectro-polarimetric techniques. Bright points are also seen on images taken in the blue continuum spectral range, but with significantly less intensity contrast as compared to the G-band. Recent radiative transfer computations on the basis of realistic MHD simulations indicate that the local brightness excess in CH filtergrams is due to the high temperature of magnetic elements at the height of line-core formation of CH molecular lines compared to the relatively field-free atmosphere (Shelyag et

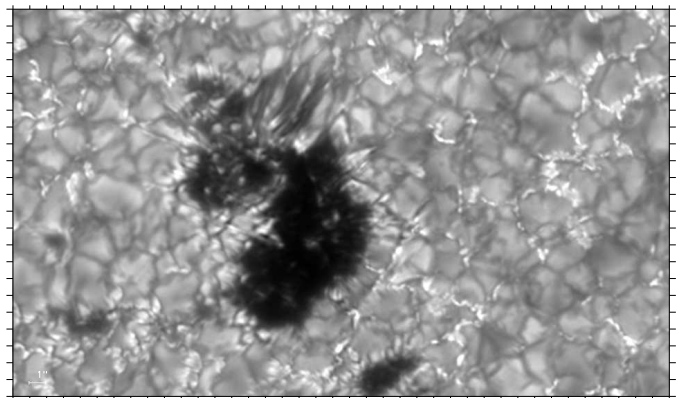


Fig. 1. Joint Phase Diversity Speckle reconstructed CN-band head image of part of an active region NOAA0669 $\mu = 0.97$ at 4.91° S, 8.14° E, taken with the SST on 7 September, 2004 at 14:30:15.

al. 2004). Numerical MHD simulations by Steiner et al. (2001) showed that another diatomic molecule in the solar atmosphere, CN, in the region $10^{-4} \leq \tau \leq 10$ behaves very similarly to CH. Computations using plane parallel model atmospheres show that the contrast values of a BP is expected to be higher in the UV band-head at 388.3 nm of CN than the in G-band (Berdyugina et al. 2003). The

typical size of BPs is around 160 km (Wiehr et al. 2004), which requires high-resolution observation techniques to spatially resolve them and to provide reliable information on their brightness distribution and structure. Early observations of active regions in the CN band head (e.g. Chapman 1970, Sheeley 1971) did not possess the necessary spatial resolution. In this paper we present a quantitative comparison between the contrast of BPs in the G-band, the CN band-head, and the blue continuum measured from high resolution filtergrams. We also compare with model predictions.

2. Observations and analysis

Observations were carried out at the new Swedish 1-m Solar Telescope (SST) on La Palma in September 2004. We observed different active regions on the Sun containing BPs in three spectral regions. Phase diversity image pairs in the CN band-head were recorded on a KODAK Megaplug 4.2 CCD camera (the field of view was reduced to 660×1050 pixels with a pixel size of $9 \mu\text{m}$) through a 0.8 nm wide interference filter centered at 388.7 nm. Phase diversity image pairs in the G-band (430.5 nm) and at 436.5 nm (blue continuum) were captured on two KODAK Megaplug 1.6 CCDs (1536×1024 pixels with a pixel size of $9 \mu\text{m}$) cameras with FWHM of 1.0 nm too. Beamsplitters enabled simultaneous recordings in the three spectral regions. In our observations the exposure time was 12 ms for CN and 11 ms for G-band and continuum. All taken filtergrams were correlated to each other.

The contrast of small-scale structures in an image is very sensitive to its spatial resolution. Although the theoretical spatial resolution of the SST at 430 nm is around 0.11 arcsec, purely diffraction limited images are not achieved directly due to wavefront aberrations of two different types: aberrations due to random fluctuations of the refractive index of the earth's atmosphere and static aberrations within the telescope itself. The tip-tilt mirror of the SST corrects for strong inclinations of the wavefront and therefore compensates for image shifts on the CCD. The Adaptive Optics system (AO) of the telescope compensates for some part of the atmospheric aberrations (Scharmer et al. 2003). However, even with this equipment the observed images were still degraded by residual atmospheric aberrations. In order to achieve nearly diffraction limited images the technique of Joint Phase Diversity Speckle (JPDS) image restoration was used (Paxman et al. 1992; Löfdahl 2002).

This method consists of collecting in each spectral region sequences of image pairs (one focused and one defocused image; phase diversity technique) at different moments within a reasonably short time interval (atmospheric realizations). This time interval must be shorter than the characteristic time scale of BP evolution. For our observations the analysis of time sequences of filtergrams did not show visible motions or structure changes of the BPs up to 100 km scales in less than 15 seconds. Therefore, to be conservative, we selected the best 8 Phase Diversity

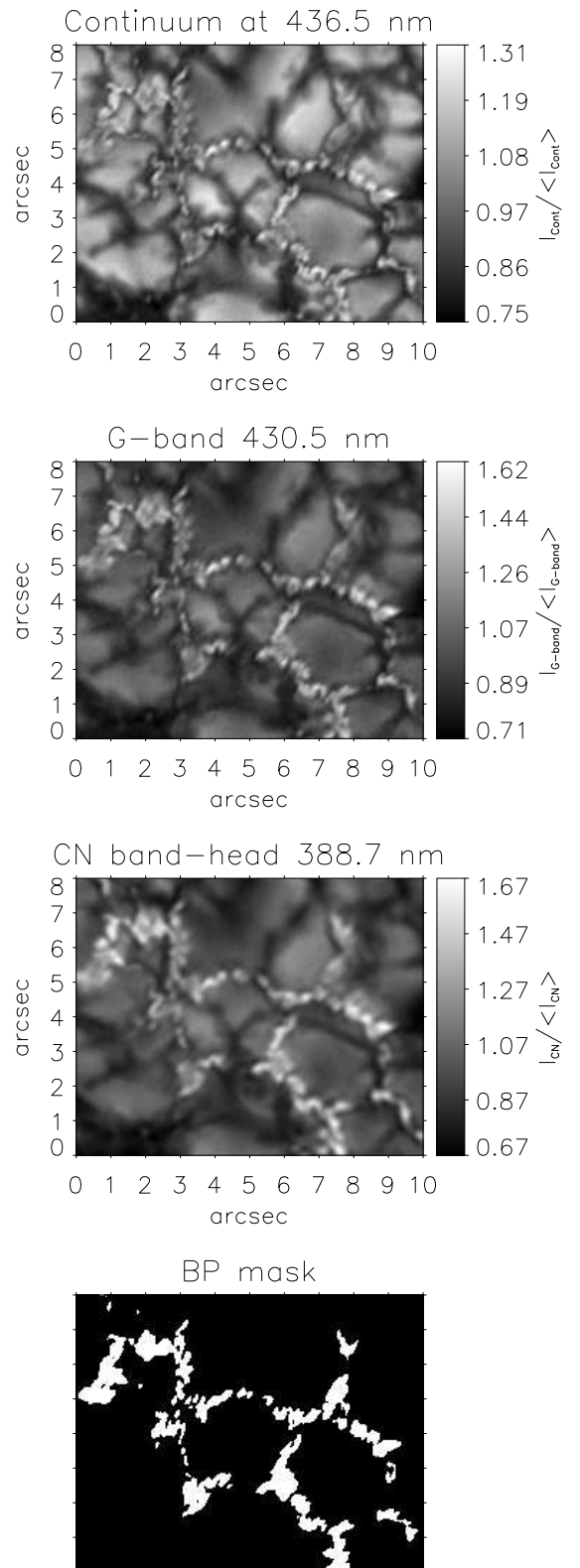


Fig. 2. Joint Phase Diversity Speckle reconstructed filtergrams containing BPs taken in the blue continuum (436.5 nm), G-band (430.5 nm) and CN band head (388.7 nm). Also shown (bottom) is the mask used to identify bright points. The plotted images have not been filtered to equalize spatial resolution

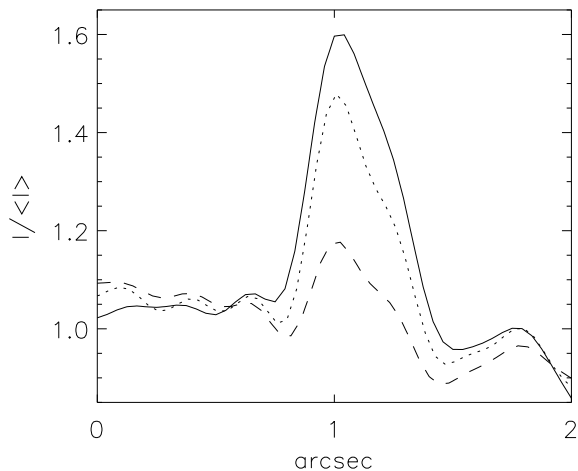


Fig. 3. Intensity along a cut through a typical BP for the blue continuum (436.5 nm - dashed line), G-band (430.5 nm - dotted line) and CN (388.7 nm - thick solid line).

image pairs obtained within 10 seconds for further investigation. The unbiased comparison of the contrast values of BPs at different wavelengths requires images with equally high spatial resolution in all three spectral regions (CN, CH and blue continuum). This is particularly problematic, since the magnitude of the residual atmospheric aberrations is wavelength dependent in an only approximately and statistically known fashion.

Deconvolution part of Phase Diversity method is very sensitive to the signal-to-noise ratio of the observed image and to its contrast. Although in theory the JPDS algorithm can yield an unaberrated image, due to photometric noise only near-diffraction limited resolution of the restored image can be achieved. The Phase Diversity algorithm assumes an isoplanar image formation process, which is not the case for image formation through the turbulent Earth's atmosphere. The algorithm is therefore usually applied to subfields smaller than or on the order of the isoplanatic angle, and a restored frame is made by mosaicking the object estimates from each subfield. For our data, 128x128-pixel subfields (corresponding to 5.2x5.2 arcsec) were used. In order to equalize the spatial resolution of the restored CN, CH, and blue continuum images the following technique was applied: in the last step of the JPDS reconstruction, for a given subfield, the final restored CN, CH and continuum subfields were filtered with the same spatial filter. This filter was based on the cut-off frequencies, in the Fourier domain, of the worst image, which always was the CN filtergram probably due to the lower S/N in the original images. This technique works if the sizes of the smallest structures lie below the spatial resolution. MHD simulations suggest that this is the case.

3. Results

In Fig. 2 reduced filtergrams in the blue continuum, G-band and CN are presented. The contrast for a given pixel assigned to a BP is defined as:

$$C_{\lambda} = \frac{I_{\lambda} - I_{0,\lambda}}{I_{0,\lambda}}, \quad (1)$$

where I_{λ} denotes the intensity of the BP in a certain wavelength band λ and $I_{0,\lambda}$ is the mean intensity of the quiet sun for the same wavelength. Intensities of BP pixels vary over a wide range. Often BP brightness is less than the brightness of granules (Langhans et al. 2002, Shelyag et al. 2004). In order to allow a secure and automated identification of BPs we use the technique of Berger et al. (1998), which consists in the subtraction of the continuum image from the corresponding G-band image.

On the bottom image in Fig. 2 regions corresponding to all BPs with an brightness 1.25 times higher than the mean intensity in the G-band, which according to Shelyag et al. (2004) corresponds to (temperature at the layer of the continuum intensity formation) $T_{\tau \approx 2/3} > 6500^{\circ}K$ are marked with black contour lines. All three reconstructed filtergrams were correlated, consequently the same BP-mask could be used. In Fig. 3 intensity cuts through a typical BP in the three spectral regions are shown. The intensities are normalized to the average quiet Sun values. The calculated mean contrast values of BPs are presented in Table 1, where $\langle C \rangle$, $\langle C^{JPDS} \rangle$ and $\langle C^{JPDS+equ} \rangle$ are the contrast in the not reconstructed, JPDS reconstructed and JPDS reconstructed with resolution equalization images respectively. The contrast of the BPs is higher in CN than in the G-band, with the mean ratio $\langle C_{CN}/C_{CH} \rangle = 1.41$. The corresponding contrast ratio of BPs as predicted by Berdyugina et al. (2003) is 1.44.

Table 1. Observed and theoretical contrast values of BPs with respect to the quiet Sun intensity within the G-band at 430.5 nm, violet CN band-head at 388.7 nm and blue continuum at 436.5 nm. Rms contrasts are computed for the quiet Sun.

Spectral region	$\langle C \rangle$	$\langle C^{JPDS} \rangle$	$\langle C_{equ}^{JPDS} \rangle$	rms
Continuum	0.090	0.145	0.143	0.11
G-band	0.218	0.341	0.340	0.12
CN	0.311	0.481	0.481	0.12

A statistical study of the brightness distributions of BPs in CN and CH filtergrams showed that the contrast ratio of the BPs in CN to CH decreases with increasing continuum brightness of the BPs (Fig. 4). In Fig. 4 only a subset of the analyzed data is shown, for a subfield for which the alignment of the various images was particularly good.

4. Conclusions

Our analysis of filtergrams of an active region in the G-band, the CN band head, and the blue continuum shows

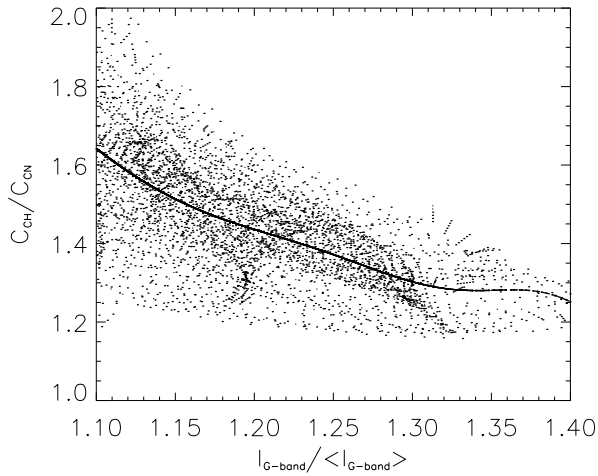


Fig. 4. Scatter plots of the contrast ratio in CN band head and G-band filtergrams vs normalized continuum (436.5 nm) intensity. The solid line represents a least square fit to the data points.

that the mean contrast value of inter-granular bright points with respect to the quiet Sun in CN is typically $C_{CN}/C_{CH} \approx 1.4$ times higher than in G-band and $C_{CN}/C_{cont} \approx 3.4$ times higher than in the blue continuum, which is in reasonable agreement with simple theoretical predictions: $C_{CN}^{theor}/C_{CH}^{theor} = 1.4$, $C_{CN}^{theor}/C_{cont}^{theor} = 2.8$ (Berdyugina et al. 2003). The contrast of BPs in the G-band is $C_{CH}/C_{cont} \approx 2.4$ times higher than in the blue continuum, also in rough agreement with their predictions: $C_{CH}^{theor}/C_{cont}^{theor} = 2.0$. Note that the absolute contrast values of observed BPs are lower than those in theoretical predictions concerning the Kurucz model with $T_{eff} = 6500^{\circ}K$ by a factor of 5. Theoretically the relative brightness excess of BPs in CN with respect to G-band is due to a stronger decreasing of the number density of the CN molecule with increasing temperature at the level of line-core formation, as compared to CH. The difference between the contrasts found from the observations and computed by (Berdyugina et al. 2003) can be attributed to several factors, the main ones of which are: 1) The computed contrasts refer to an unlimited spatial resolution whereas our observed filtergrams are limited to a spatial resolution of 130 km; 2) the observed contrast is further diminished by scattered light. Alternatively, the temperature contrast between magnetic BPs and the quiet Sun is lower. The significantly lighter contrast seen in the violet CN band-head compared with the G-band makes it a promising wavelength band for solar high resolution studies. Detailed synthesis of this wavelength band using 3-D MHD simulations would also be of interest.

5. Acknowledgements

The NSST is operated by the Swedish Royal Academy of Sciences at the Spanish Observatorio del Roque de los Muchachos of the Instituto de Astrofísica de Canarias.

References

- Berdyugina, S.V., Solanki, S.K., and Frutiger, C. 2003, *A&A*, 412, 513
- Berger, T.E., & Title, A.M. 1996, *ApJ*, 463, 365
- Berger, T.E., Löfdahl, M.G., Title, A.M., & Shine, R.S. 1998, *ApJ*, 495, 973 (Paper II)
- Chapman, G.A. 1970, *Sol.Phys.*, 18, 78
- Langhans, K., Schmidt, W., & Tritschler, A. 2002, *A&A*, 394, 1069
- Löfdahl, M.G. 2002, in *Proc. SPIE*, Vol. 4792, Image Reconstruction from Incomplete Data II, ed. P.J. Bones, M.A. Fiddy and R.P. Millane, 146
- Löfdahl, M.G., Berger, T.E., Shine, R.S., & Title, A.M. 1998, *ApJ*, 495, 965
- Muller, R., & Roudier, T. 1984, *Sol. Phys.*, 94, 33
- Paxman, R.G., Schulz, T.J., & Fienup, J.R. 1992, *Journal of the Optical Society of America*, 9(7), 1072
- Scharmer, G.B., Dettori, P.M., Peter, M., Löfdahl, M.G., Shand, M. 2003, *SPIE*, Vol. 4853, 370
- Sheeley, N.R. 1971, *Sol.Phys.*, 20, 19
- Shelyag, S., Schüssler, M., Solanki, S. K., Berdyugina, S. V., and Vögler, A. 2004, *A&A*, 427, 335
- Steiner, O., Hauschildt, P., Bruls, J. 2001, *A&A*, 372, 13
- Steiner, O., Hauschildt, P., and Bruls, J. 2003, *Astron. Nachr.*, 324, 398
- Wiehr, E., Bovelet, B., and Hirzberger, J. 2004, *A&A*, 422, 63